

time-of-flight mass spectrometry (MALDI-TOF-MS; see Figure S2). Peptide L1 alone adopts a random-coil conformation in aqueous solution (100 μM , $\text{pH} \approx 6.0$), as observed from circular dichroism (CD) spectra, which showed with a strong negative band at 199 nm and a very weak positive band at 207 nm (Figure 2). However, a bisignate positive band at 197 nm together with a negative Cotton effect at 214 nm were observed in CD spectra (Figure 2) upon the addition of $\text{H}_4\text{SiW}_{12}\text{O}_{40}$ (HSiW, Figure 1b) to an aqueous solution of L1, thus demonstrating the commencement of a conformation transition from a random-coil to a β -sheet state.^[13] The intensity of the negative signal at 214 nm increased gradually until a maximal β -sheet content was reached with a molar ratio of L1 to HSiW ($M_{\text{L1/HSiW}}$) near 2:1. A further increase in the stoichiometry of HSiW led to precipitation of the material and thereby the disappearance of the CD signal.

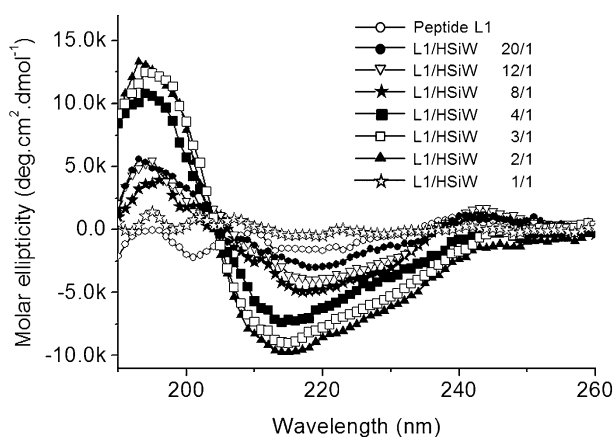


Figure 2. CD spectra of peptide L1 and the L1/HSiW composites with different molar ratios in aqueous solution (the concentration of L1 in all the CD samples was fixed at 100 μM).

When a solution of L1 was cast onto a copper grid and then negatively stained with uranyl acetate, irregular spherical structures (Figure 3a) with a size of 20–40 nm were observed by transmission electron microscopy (TEM). In great contrast, well-separated one-dimensional (1D) nanofibers were observed after the mixing of L1 with HSiW in water even at $M_{\text{L1/HSiW}}$ ratios below 8:1 (see Figure S3) or peptide concentrations above 10 μM (see Figure S4). As a representative example, the TEM image of L1/HSiW with a $M_{\text{L1/HSiW}}$ ratio of 3:1 is shown in Figure 3b. Uniform nanofibers with a diameter of (13 ± 1) nm and lengths reaching several micrometers can be observed. The strong electronic contrast of the nanofibers is thought to originate from the electron-dense HSiW clusters and the densely packed azobenzene units, since no contrasting agent was used during the preparation of the TEM specimens of the nanofibers. This hypothesis was validated by UV/Vis and energy-dispersive X-ray (EDX) spectra. The UV/Vis absorption band of azobenzene units in the L1/HSiW solution showed a hypsochromic shift as compared with that of individual L1 (see Figure S5), thus indicating that the azobenzene units of the ionically self-assembled samples form a densely packed state as a result of the hydrophobic and/or π - π interactions. EDX spectra of the

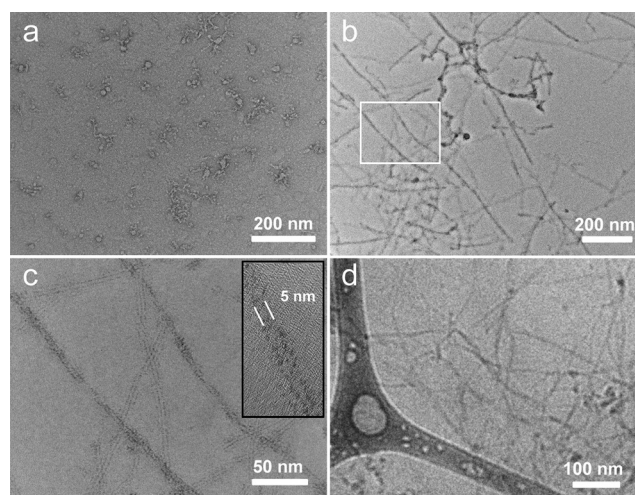


Figure 3. Morphological studies of the individual peptide L1 and the L1/HSiW (3:1) composite: a) TEM image of L1; b) TEM image of L1/HSiW; c) high-resolution TEM image of L1/HSiW for the area in (b) defined by the white rectangle; d) cryo-TEM image of L1/HSiW.

nanofibers showed the presence of elemental tungsten derived from the HSiW clusters (see Figure S6).

Isothermal titration calorimetry (ITC; see Figure S7) proved that the ionic self-assembly process between L1 and HSiW has a large exothermicity ($\Delta H = (-99.12 \pm 0.54)$ kJ mol^{-1}) and is associated with a high binding constant ($K_a = (6.12 \pm 0.22) \times 10^7 \text{M}^{-1}$), thus implying that the main driving force is strong electrostatic attraction. FT-IR (see Figure S8b) and ^{183}W NMR spectra (see Figure S9) showed that the HSiW cluster remained stable during the ISA process. Similar nanofibers were also observed when L1 was mixed with other polyanionic clusters, such as $\text{Na}_3\text{AlMo}_6(\text{OH})_6\text{O}_{18}$ or $\text{Na}_6\text{V}_{10}\text{O}_{28}$ clusters (see Figure S10). High-resolution TEM (Figure 3c) revealed that the HSiW nanoclusters (black dots) formed a double-layer arrangement within the nanofibers with a layer distance of (5 ± 1) nm. Cryogenic TEM (cryo-TEM; Figure 3d) and thioflavin T (ThT) titration (see Figure S11) provided further evidence that long nanofibers with extended β -sheet structures existed in aqueous solution, and that their formation was not caused by the drying effect during the solvent-evaporation process. Zeta-potential measurement revealed that the resultant aqueous nanofibers had a net potential of +43 mV (see Figure S12), thus implying that the surface of the nanofibers was covered by highly concentrated positive segments.

Considering the molecular length ($l \approx 2.0$ nm) of β -sheet L1 between the hydrophilic amine at the ϵ -position of lysine and the azobenzene unit, the 1 nm diameter of HSiW, the 13 nm width of the nanofibers, the 5 nm distance of the double-layer HSiW, and the positive zeta potential, we propose that the nanofibers possess a core-shell structure. Peptides are electrostatically connected by HSiW to form a primary sandwich fragment, and two laterally contiguous sandwich fragments stack further to form a fibrillar core (Figure 1b). Meanwhile, the excess peptide molecules ($M_{\text{L1/HSiW}}$ is 3:1) adsorb to the surface of the fibrillar core with protonated lysine groups toward the outside, thus acting as

a shell to stabilize the fibrillar core in water. It is clear that the electrostatic attraction between L1 and HSiW initiates the conformational evolution of L1 from the random-coil to the β -sheet state. The directional hydrogen bonding of the β -sheet peptide backbones together with the strongly hydrophobic interaction and/or π - π stacking of planar azobenzene side groups then provide additional energetic contributions for the formation of 1D extended nanostructures.

The aqueous nanofibers are photosensitive because of the conformational transition of azobenzene side groups upon UV irradiation (see Figure S13). This *trans*-to-*cis* conformational transition forced the long nanofibers to break up into short nanostructures and subsequently form aggregates within 1 day (see Figure S14). This phenomenon suggests that the nonplanar *cis* azobenzene units with an increased steric effect not only block the extending 1D stacking of peptides but also cause the disassociation of the shell peptides from the surface of the core. The broken fibrillar core with its hydrophobic surface exposed to water is unstable and has a strong propensity to coagulate into insoluble aggregates.

To further shed light on the effect of hydrophobic residues on the self-assembled nanostructures, we designed two analogous peptides, L2 and L3. Peptides L2 and L3 were synthesized by replacing all the azobenzene side segments of L1 with phenylalanine and valine residues, respectively (Figure 1 a). As compared to L1, this molecular design of L2 and L3 should offer reduced hydrophobic and/or π - π interactions. TEM measurements showed irregular nanospheres after HSiW was mixed with L2 or L3 (see Figure S15). These spherical nanostructures are unstable and turn into precipitates (see Figure S15). This situation led us to conclude that peptides with less hydrophobic residues are unfavorable for both the 1D molecular stacking and the stability of the resultant nanostructures. With this hypothesis in mind, we further synthesized additional peptides with shorter hydrophobic sequences (L4 and L5) and longer hydrophobic sequences (L6 and L7) to compare their ionic self-assembly behavior. As expected, unstable spheres were observed after the mixing of HSiW with L4 or L5 (see Figure S15). Peptide L6 with four phenylalanine residues also formed unstable nanospheres upon the addition of HSiW (see Figure S15). However, peptide L7 with four azobenzene side groups again formed stable 1D nanofibers after mixing with HSiW. Our results indicate that strong hydrophobic and/or π - π interactions between the peptides not only facilitate the formation of 1D nanostructures but also improve their stability in water.

These stable L1/HSiW nanofibers with positively charged surfaces are multivalent candidates for binding with bacterial cells. The antimicrobial activity of the L1/HSiW nanofibers was explored with the ubiquitous and clinically relevant bacterium *Escherichia coli*. Profiling against *E. coli* in a broth dilution assay in the presence of L1/HSiW nanofibers was monitored by measuring the incubation-time-dependent optical density (OD_{600}). For comparison purposes, *E. coli* samples treated with individual L1 and HSiW were used as references. The data are expressed as the mean and standard deviation of at least three replicates. The standard deviation is shown by the error bars. The inhibitory ability of L1 or HSiW alone was poor (Figure 4). However, the L1/HSiW nanofibers

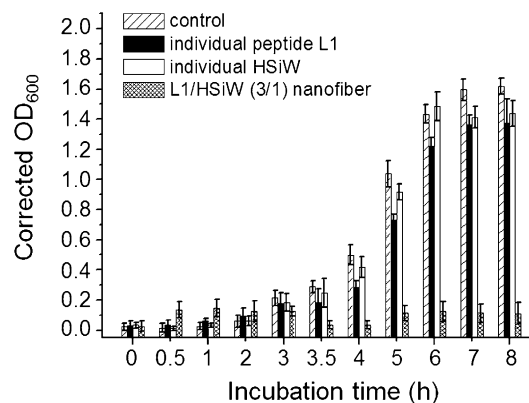


Figure 4. Optical density of *E. coli* with incubation time in the presence of the individual peptide L1, individual HSiW, and L1/HSiW nanofibers (the concentrations of L1 and HSiW in all the samples were kept at 60 and 26.7 μ M, respectively).

exhibited significantly enhanced antibacterial efficacy. Correspondingly, the reduced turbidity of the *E. coli* sample incubated with the nanofibers revealed a reduction in cell viability (see Figure S16). The dose-dependent growth inhibition of *E. coli* suggests that the minimal inhibitory concentration (MIC) of the peptide nanofibers is 60 μ M (see Figure S17).

To gain more insight into the mechanism by which nanofibers exert their activity, we performed a dead assay for cell viability. In this assay, *E. coli* cells were mixed with the L1/HSiW nanofibers and incubated for 14 h under growth conditions. Then, the dye propidium iodide (PI) was added. PI molecules, which display red fluorescence, can only penetrate the plasma membrane of dead cells whose membranes have been compromised.^[26] Laser scanning confocal microscopy showed that the *E. coli* cells that were not incubated with the nanofibers were fluorescence-silent (see Figure S18a). In great contrast, red-fluorescing samples were observed after the treatment of *E. coli* cells with L1/HSiW nanofibers (see Figure S18b). This result strongly suggests that *E. coli* cells undergo cell death through a mechanism that involves cell-membrane disruption upon contact with the nanofibers.^[27] Besides *E. coli* cells, the multivalent nanofibers also displayed effective inhibition against yeast cells (see Figure S19).

It has been proposed that the activity of antibacterial peptides follows three consecutive steps: 1) the electrostatic binding of cationic peptides to the cell membrane; 2) accumulation of the peptides on the surface of the cell membrane; and 3) the insertion of concentrated peptides into the cell membrane to induce cell lysis.^[28,29] Some recent reports demonstrated that the antibacterial efficacy could be improved significantly when cationic peptides self-assembled into large aggregates, since the concentration of lysine groups can dramatically enhance the binding affinity through multiple simultaneous interactions with bacterial membranes.^[8,30,31] However, we herein propose an alternative possibility that the large peptide aggregates not only strengthen the binding avidity, but also avoid the slow accumulation process of individual peptides (the accumulation of peptide molecules on the surface of bacteria—the second step stated above—is

a slow thermodynamic process). These two factors may work together to contribute to the enhanced antibacterial efficacy.

Another important feature of the nanofibers is their resistance to enzyme degradation in human sera. Whereas the individual peptide L1 showed rapid degradation ($t_{1/2} \approx 3$ h; see Figure S20), L1/HSiW nanofibers showed excellent stability: partial degradation (<20%) was observed after 6 h of incubation, and their half-life was estimated to be approximately 15 h. This result strongly demonstrated that ionic self-assembly was a prerequisite for stabilizing the cationic peptide L1. The improved resistance of the nanofibers to enzymatic degradation could prolong their life span in the circulation and facilitate their delivery to target tissue in the future.

In conclusion, we have demonstrated that multiple electrostatic interactions between polyoxometalates and short peptides could be utilized to generate multivalent nanofibers. Hydrophobic and/or π - π interactions between the peptides were strong enough to enable the formation of stable 1D nanostructures. Because of the supramolecular nature of the ensemble, POMs thus enabled the enhancement of the antimicrobial efficacy and biological stability of short peptides in situ. Although the present study has focused on antibacterial activity, it is also expected that the extraordinary properties of POMs could be used to create hierarchical assemblies of value for the fields of biological chemistry and materials science.

Acknowledgements

This research was supported by the NSFC (21573091), the National Basic Research Program (2013CB834503), and the Sci-Tech development project of Jilin Province (20130522133JH).

Keywords: bioactivity · ionic self-assembly · multivalent nanofibers · polyoxometalates · short peptides

How to cite: *Angew. Chem. Int. Ed.* **2016**, *55*, 2592–2595
Angew. Chem. **2016**, *128*, 2638–2641

-
- [1] A. G. Cherstvy, *Phys. Chem. Chem. Phys.* **2011**, *13*, 9942–9968.
 [2] H. Schiessel, *J. Phys. Condens. Matter* **2003**, *15*, R699–R774.
 [3] R. H. Mo, J. L. Zaro, W.-C. Shen, *Mol. Pharm.* **2012**, *9*, 299–309.
 [4] S. Faham, R. E. Hileman, J. R. Fromm, R. J. Linhardt, D. C. Rees, *Science* **1996**, *271*, 1116–1120.
 [5] B. J. Zern, H. Chu, A. O. Osunkoya, J. Gao, Y. Wang, *Adv. Funct. Mater.* **2011**, *21*, 434–440.
 [6] D. Zaramella, P. Scrimin, L. J. Prins, *J. Am. Chem. Soc.* **2012**, *134*, 8396–8399.
 [7] X. Xu, Y. Jian, Y. Li, X. Zhang, Z. Tu, Z. Gu, *ACS Nano* **2014**, *8*, 9255–9264.
 [8] L. Liu, K. Xu, H. Wang, J. Tan, P. K. J. Tan, W. Fan, S. S. Venkatraman, L. Li, Y.-Y. Yang, *Nat. Nanotechnol.* **2009**, *4*, 457–463.
 [9] P. Chairatana, E. M. Nolan, *J. Am. Chem. Soc.* **2014**, *136*, 13267–13276.
 [10] S. Bulut, T. S. Erkal, S. Toksoz, A. B. Tekinay, T. Tekinay, M. O. Guler, *Biomacromolecules* **2011**, *12*, 3007–3014.
 [11] M. Yolamanova, C. Meier, A. K. Shaytan, V. Vas, C. W. Bertocini, F. Arnold, O. Zirafi, S. M. Usmani, J. A. Müller, D. Sauter, C. Goffinet, D. Palesch, P. Walther, N. R. Roan, H. Geiger, O. Lunov, T. Simmet, J. Bohne, H. Schrezenmeier, K. Schwarz, L. Ständker, W.-G. Forssmann, X. Salvatella, P. G. Khalatur, A. R. Khokhlov, T. P. J. Knowles, T. Weil, F. Kirchhoff, J. Münch, *Nat. Nanotechnol.* **2013**, *8*, 130–136.
 [12] L. Chen, J. F. Liang, *Biomacromolecules* **2013**, *14*, 2326–2331.
 [13] I. Choi, I.-S. Park, J.-H. Ryu, M. Lee, *Chem. Commun.* **2012**, *48*, 8481–8483.
 [14] P. Wadhvani, E. Strandberg, N. Heidenreich, J. Bürck, S. Fanghänel, A. S. Ulrich, *J. Am. Chem. Soc.* **2012**, *134*, 6512–6515.
 [15] V. A. Kumar, S. Shi, B. K. Wang, I.-C. Li, A. A. Jalan, B. Sarkar, N. C. Wickremasinghe, J. D. Hartgerink, *J. Am. Chem. Soc.* **2015**, *137*, 4823–4830.
 [16] K. Liu, R. R. Xing, C. J. Chen, G. Z. Shen, L. Y. Yan, Q. L. Zou, G. H. Ma, H. Möhwald, X. H. Yan, *Angew. Chem. Int. Ed.* **2015**, *54*, 500–505; *Angew. Chem.* **2015**, *127*, 510–515.
 [17] S.-T. Chou, K. Hom, D. Zhang, Q. Leng, L. J. Tricoli, J. M. Hustedt, A. Lee, M. J. Shapiro, J. Seog, J. D. Kahn, A. J. Mixson, *Biomaterials* **2014**, *35*, 846–855.
 [18] H. N. Miras, J. Yan, D. L. Long, L. Cronin, *Chem. Soc. Rev.* **2012**, *41*, 7403–7430.
 [19] D. Y. Du, J. S. Qin, S.-L. Li, Z. M. Su, Y. Q. Lan, *Chem. Soc. Rev.* **2014**, *43*, 4615–4632.
 [20] T. Yamase, *J. Mater. Chem.* **2005**, *15*, 4773–4782.
 [21] H. Stephan, M. Kubeil, F. Emmerling, C. E. Müller, *Eur. J. Inorg. Chem.* **2013**, 1585–1594.
 [22] I. S. Lee, J. R. Long, S. B. Prusiner, J. G. Safar, *J. Am. Chem. Soc.* **2005**, *127*, 13802–13803.
 [23] J. Geng, M. Li, J. S. Ren, E. B. Wang, X. G. Qu, *Angew. Chem. Int. Ed.* **2011**, *50*, 4184–4188; *Angew. Chem.* **2011**, *123*, 4270–4274.
 [24] X. H. Yan, P. L. Zhu, J. B. Fei, J. B. Li, *Adv. Mater.* **2010**, *22*, 1283–1287.
 [25] V. Goovaerts, K. Stroobants, G. Absillis, T. N. Parac-Vogt, *Phys. Chem. Chem. Phys.* **2013**, *15*, 18378–18387.
 [26] A. W. Thomas, Z. B. Henson, J. Du, C. A. Vandenberg, G. C. Bazan, *J. Am. Chem. Soc.* **2014**, *136*, 3736–3739.
 [27] D. A. Salick, J. K. Kretsinger, D. J. Pochan, J. P. Schneider, *J. Am. Chem. Soc.* **2007**, *129*, 14793–14799.
 [28] I. M. Herzog, M. Fridman, *MedChemComm* **2014**, *5*, 1014–1026.
 [29] E. Terzi, G. Hölzemann, J. Seelig, *Biochemistry* **1997**, *36*, 14845–14852.
 [30] J. Chen, F. Wang, Q. Liu, J. Z. Du, *Chem. Commun.* **2014**, *50*, 14482–14493.
 [31] L. Chen, N. Patrone, J. F. Liang, *Biomacromolecules* **2012**, *13*, 3327–3333.

Received: December 4, 2015

Published online: January 14, 2016